

Drill String Modeling and Stress Analysis

A. Abdul-Ameer

Abstract— The unsupported deflection of drill strings which are subjected to increasing gravitational loading and distortion, with borehole depth and twisting, is considered. Eccentric loading configurations which include the lateral reaction to mud flow pressure, compression, bending forces and twisting moments are incorporated in the derivations. The bending- buckling deflections and twist angle dynamics following drill string drive motor voltage changes are provided. The principal stress level is identified when operating at particular borehole depths and with specified cutting velocities.

Index Terms— deflections, drill, principal, stresses, strings

I. INTRODUCTION

DURING oil and natural gas, borehole drilling operations, there are many engineering problems to contend with, as discussed in [1], including the failure of the drill string (ds) owing to the combined compression, buckling and torsional stresses encountered. Moreover, as a result of the cutting action of the drill bit, as rock with a variety of physical properties is penetrated, stochastic loading on the ds is excited leading to the possibility of fatigue failure, permanent dynamic, spiral twisting, vibration and buckling deformation.

Further difficulties may arise with the onset of loading misalignment eccentricity, when buckling and twisting may cause contact between the borehole rock face and the ds circumference. This and the gyroscopic couple, due to the cutting head rotation, as discussed in [2], may also lead to additional lateral loading and ds rupture.

The main feature of borehole drilling arises from the extreme slenderness ratio (effective length/ radius of gyration) of the ds column with the torque on bit (tob) applied at the top of the column. As a result of this, the ds mass and hence the gravitational force on the rock to be penetrated, known as the weight on the drill bit (wob), steadily increases. This is due to the number of tubular steel ds sections employed which often exceed 1000 m in length, when assembled.

These extreme conditions and the objective of exercising closed loop computer regulation, for oil and gas exploration, provide the motivation for this study. However, before automatic control can be embarked upon, accurate models, replicating drilling operations and procedures enabling the determination of the stresses encountered, require formulating.

In this study, as a prelude to further combined compression, bending and twisting investigations, emphasis will be

focused on the bending/ buckling and twisting problems owing to the vertical, eccentric, steadily increasing gravitational loading on the drill bit and the torsional moment applied at the apex of the ds.

The techniques advocated, include the bending and twisting effects originating from the external pressurized ds mud flow which is employed to clear rock debris from the cutting head. Consequently, in this initial viability study, emphasis will remain on the bending / twisting problem and on the solutions to the unsupported, lumped- distributed torsional and buckling deflection equations enabling the identification of the principal stress levels, before the employment of stabilizers.

II. BUCKLING

The pioneering approach to ds buckling was undertaken by [3] with analysis procedures which considered the shear forces acting on a ds column. Later work by [4] considered the buckling and lateral vibrations of the ds in efforts to extend earlier research. More recently, the fatigue problem arising from ds bending and twisting was investigated in [5] using FE methods.

In the analysis herein, only the principal loading components are considered together with the lateral effects from the pressurized mud flow following ds bending.

Although drill strings are subjected to combined buckling, twisting and compressive loading resulting in complicated, longitudinal, three dimensional spiral deformations when unrestricted, in practice the ds contact with the concentric, borehole rock face, confines these deflections. In fact, before this contact is established, stabilizers are usually employed to limit lateral deflections and the prospect of ds shearing.

Consequently, the prediction of the maximum deflection of the ds and the axial location of this maximum, for a specific borehole depth, is important. Once this maximum, lateral deflection equals the borehole diameter, before lining, the use of stabilizer supports becomes necessary.

In this study the increasing gravitational load arising from the lengthening ds, before the use of stabilizers, to resist ds lateral deformation, will be investigated. With this loading configuration the task is to determine the ds deflections, $y(z)$ and $\theta(z)$, respectively, where z is the depth down the borehole, $0 < z < L$ and L is the cutting bit depth.

A. Buckling Analysis

In this section, the ds drive axis will be assumed to be a distance e from the vertical axis of the ds cutting head, as shown in Fig. 1. Consequently, with the gravitational loading at depth z of, $g\rho Az$ arising from the advancing ds mass c of g , bending- buckling of the ds would be inevitable.

Manuscript received June 18, 2012; revised July 26, 2012. This work was supported in part by the British University in Dubai, research grant ENG009.

Dr A. Abdul-Ameer, Author is an Associate Professor in Systems Engineering at the British University in Dubai, P.O. Box 345015, Dubai-UAE, phone: +971-43602905; fax: +971-43664698; e-mail: alaa.ameer@buid.ac.ae).

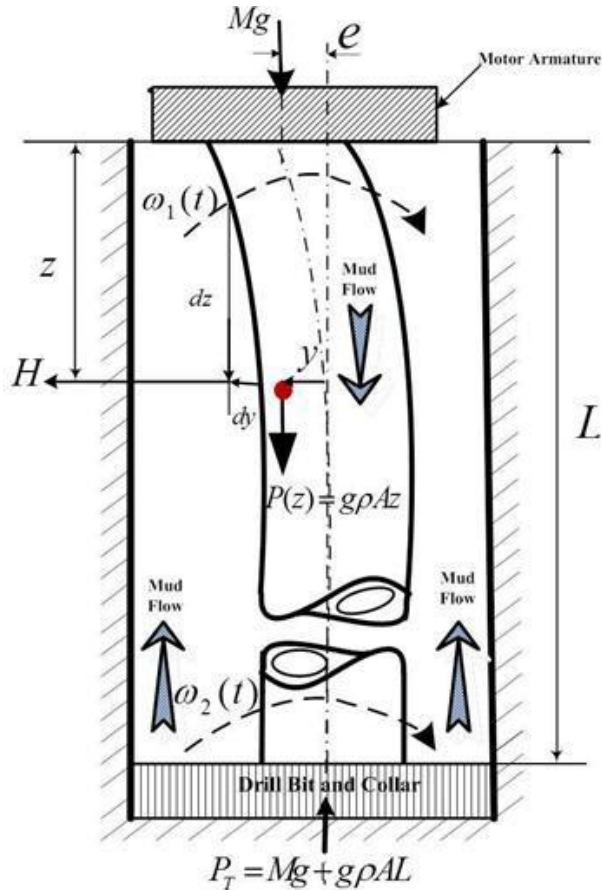


Fig. 1, Drill String and Borehole Representation

Considered in this way the problem of buckling reduces to determining how much the ds column could be allowed to bend, before employing stabilizers, to constrain this deflection.

The use of established procedures requires the induction of a complementary, harmonic function and a particular integral, see for example [6], governing the ds deflection curve, $y(z)$, to achieve a solution. Unfortunately, the increasing gravitational loading arising from the steadily advancing ds length, inhibits this approach inviting thereby a polynomial, series assessment for $y(z)$, as considered in [7].

In accordance with the free body diagram of Fig. 1, the bending moment equation is:

$$\bar{M} = -Hz \frac{dy}{dz} - P(z)y(z) - Mge \quad (1)$$

where in (1) $P(z)$ is the increasing gravitational force, so that at depth z :

$$P(z) = g\rho Az$$

and the ds motor and coupling, gravitational force is Mg , e is the loading eccentricity, and $-Hz dy/dz$ is the mud flow, lateral component of the bending moment \bar{M} , respectively. This effect varies with the borehole depth z changing the ds slope and distorting the ds-borehole hydraulic annulus which results in an increasing, lateral moment on the ds.

At zero depth ($z=0$) this distorting moment would be zero, whereas at 1000m the hydraulic pressure would be approximately 103.4 bar (1500 lb_f/in²).

The equation for the elastic ds curve is:

$$\frac{d^2 y(z)}{dz^2} = \frac{\bar{M}}{IE}$$

Hence, substituting for (1):

$$\frac{d^2 y(z)}{dz^2} + \frac{Hz}{IE} \left(\frac{dy(z)}{dz} \right) + \frac{P(z)}{IE} y(z) = - \left(\frac{F}{IE} \right) e \quad (2)$$

where in (2):

E = modulus of elasticity

I = moment of inertia

$F = Mg$

$P(z) = g\rho Az$

and H = lateral bending moment at z .

Hence, (2) can be written as:

$$\frac{d^2 y(z)}{dz^2} + Rz \left(\frac{dy(z)}{dz} \right) + kzy(z) = -Fe \quad (3)$$

where in (3): $k = g\rho \frac{A}{IE}$ and $R = \frac{H}{IE}$.

A solution for (3), in accordance with [8], is proposed as:

$$y(z) = a_2 z^2 + a_1 z + a_0 \quad (4)$$

with boundary conditions of:

$$y(0) = -e \text{ and } y(L) = 0 \quad (5)$$

Equation (3), together with the boundary conditions may be written as:

$$\begin{bmatrix} kz^3 + 2Rz^2 + 2 & kz^2 + Rz & kz \\ 0 & 0 & 1 \\ L^2 & L & 1 \end{bmatrix} \begin{bmatrix} a_2 \\ a_1 \\ a_0 \end{bmatrix} = - \begin{bmatrix} Mg \\ 1 \\ 0 \end{bmatrix} e \quad (6)$$

Clearly, proposing any $y(z)$ of greater degree would not provide a unique solution for the coefficients a_0, a_1 and a_2 , in consideration of (6) and the boundary conditions, stated in (5).

The proposition implied by (4) reflects the theory of Frobenius F.G, given in [8] which state that (3) will have at least one solution of the form:

$$y(z) = z^m \sum_{n=0}^{\infty} a_n z^n \quad (7)$$

Inverting (6) and multiplying by the loading – boundary condition vector yields:

$$a_2 = \left[\frac{e(FL + kz^2 + Rz - kzL)}{L(-kz^3 - 2Rz^2 - 2 + Lkz^2 + LRz)} \right]$$

$$a_1 = \left[\frac{e(FL^2 + kz^3 + 2Rz^2 + 2 - kzL^2)}{L(-kz^3 - 2Rz^2 - 2 + Lkz^2 + LRz)} \right] \quad (8)$$

$$a_0 = -e$$

Substituting for a_2, a_1 and a_0 in (4) results in:

$$y(z) = \left[\frac{-z^2 e(FL + kz^2 + Rz - kzL) + ze(FL^2 + kz^3 + 2Rz^2 + 2 - kzL^2)}{L(-kz^3 - 2Rz^2 - 2 + Lkz^2 + LRz)} \right] \quad (9)$$

$-e, 0 < z < L$

B. An Upper Bound for H

In view of the effective length $L \gg 0$, selecting $z \leq 1$ would result in conditions similar to those at $z = 0$. Thus:

$$\frac{d^2 y}{dz^2} = 0, \quad \frac{dy}{dz} = -\frac{e}{L} \text{ and } y = -e$$

Then from (2):

$$H \left(-\frac{e}{L} \right) + g\rho A(-e) = -Mge \quad (10)$$

enabling an upper bound to be established for H .

III. BUCKLING APPLICATION STUDY

In this section the buckling locations, for a 1000 m ds with loading eccentricity (e) of 0.01 m, will be investigated. The ds standard dimensions of 16.82 cm (6.625") outside diameter and 12.7 cm (5") inside diameter have been accepted leading to:

$$k = g\rho \frac{A}{IE} = 13.3875 \times 10^{-5}$$

where:

$$ds \text{ cross sectional area } (A) = 2.3587 \times 10^{-3} \text{ m}^2,$$

$$\text{density of steel } (\rho) = 7800 \text{ kg/m}^3,$$

$$ds \text{ polar moment of inertia } (I) = \frac{\pi}{64} (d_o^4 - d_i^4) = 0.2652 \times 10^{-4},$$

$$\text{gravity acceleration } (g) = 9.81 \text{ m/sec}^2$$

$$\text{motor gravitational load } (Mg) = 0.13 \times 10^{-3} \text{ N}$$

$$\text{and modulus of elasticity of steel } (E) = 200 \text{ GPa.}$$

In accordance with (10): $0 < R < 0.05$

for this particular loading configuration.

As shown in Fig. 2 the curves for $R=0.01$ and $Mg/IE=0.26 \times 10^{-3}$, 1.3×10^{-3} and 2.6×10^{-3} . The buckling deflections occur at a depth of approximately 920m. In heavy, pressurized mud the ds bending dynamics would be over damped. A loading delay of 10 - 20 seconds is normally incorporated to avoid transient shock loads on the ds. This provision is included in the principal stress computation problem, developed in Section 6.

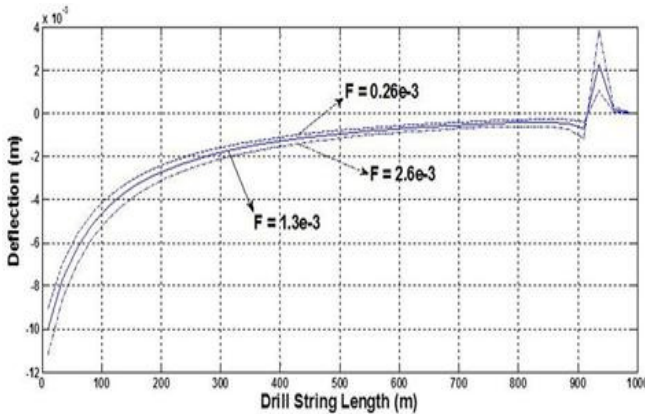


Figure 2, Drill String Bending Deflection Curves

$$k = 13.38875 \times 10^{-5}, R = 0.01, F = \frac{Mg}{IE}$$

IV. THE DISTRIBUTED PARAMETER MODELLING OF DRILL STRINGS IN TORSION

In this section, the ds will be modeled as a distributed parameter shaft, as shown in [9], with rotational inertias and viscous damping, represented by lumped parameter models, at the ds extremities.

$$\begin{bmatrix} T_1(s) \\ T_2(s) \end{bmatrix} = \begin{bmatrix} \zeta_1 w_1(s) & -\zeta_1 (w_1^2(s)-1)^{1/2} \\ \zeta_1 (w_1^2(s)-1)^{1/2} & -\zeta_1 w_1(s) \end{bmatrix} \begin{bmatrix} \omega_1(s) \\ \omega_2(s) \end{bmatrix} \quad (11)$$

In (11), and if:

$$L_1 = \rho_1 J_s, \text{ and } C_1 = \frac{1}{(G_1 J_s)^{1/2}}$$

$$\text{then: } \zeta_1 = \sqrt{\frac{L_1}{C_1}} = J_s \sqrt{\rho_1 G_1}$$

$$\text{Also: } w_1(s) = \frac{e^{2\zeta_1 \Gamma_1(s)} + 1}{e^{2\zeta_1 \Gamma_1(s)} - 1} \quad (12)$$

where in (12):

$$\Gamma_1(s) = s\sqrt{L_1 C_1} = s\sqrt{\rho_1 / G_1}$$

If in (1): $T_2(s) = R\omega_1(s)$

then following the inversion of (11):

$$\begin{bmatrix} \omega_1(s) \\ \omega_2(s) \end{bmatrix} = \frac{\begin{bmatrix} \zeta_1 w_1(s) & \zeta_1 (w_1^2(s)-1)^{1/2} \\ \zeta_1 (w_1^2(s)-1)^{1/2} & \zeta_1 w_1(s) \end{bmatrix}}{\zeta (w(s)R + \zeta)} \begin{bmatrix} T_1(s) \\ 0 \end{bmatrix} \quad (13)$$

and in delay form:

$$w_1(s) = \frac{(1 + e^{-2\zeta_1 \Gamma_1(s)})}{(1 - e^{-2\zeta_1 \Gamma_1(s)})}$$

Completing the ds torsional analysis.

V. DRILL STRING TORSIONAL MODEL

The arrangement, for analysis purposes, is shown in Fig. 3, where the motor armature and cutting head will be incorporated as rigid, lumped parameter, point wise units. Owing to the dimensions of the ds, this component will be described as a distributed parameter element, where the ds inertia and stiffness are continuous functions of ds length. The notation employed in [10], will be adopted.

In accordance with Fig. 1, (1), the Laplace transformed model for the distributed-lumped parameter description is:

$$\begin{bmatrix} T_1(s) - J_1 s \omega_1(s) - c_1 \omega_1(s) \\ J_2 s \omega_2(s) + c_2 \omega_2(s) + T_2(s) \end{bmatrix} = \begin{bmatrix} \zeta_1 w_1(s) & -\zeta_1 (w_1^2(s)-1)^{1/2} \\ \zeta_1 (w_1^2(s)-1)^{1/2} & -\zeta_1 w_1(s) \end{bmatrix} \begin{bmatrix} \omega_1(s) \\ \omega_2(s) \end{bmatrix}$$

Since $T_2(s)$ in this application is zero the impedance description becomes:

$$\begin{bmatrix} T_1(s) \\ 0 \end{bmatrix} = \begin{bmatrix} \zeta_1 w_1(s) + \gamma_1(s) & -\zeta_1 (w_1^2(s)-1)^{1/2} \\ \zeta_1 (w_1^2(s)-1)^{1/2} & -\zeta_1 w_1(s) - \gamma_2(s) \end{bmatrix} \begin{bmatrix} \omega_1(s) \\ \omega_2(s) \end{bmatrix} \quad (14)$$

In (14):

$$\gamma_1(s) = J_1 s + c_1, \quad \gamma_2(s) = J_2 s + c_2$$

$$L_1 = \rho_1 J_s, \text{ and } C_1 = \frac{1}{(G_1 J_s)}$$

and ζ , $w(s)$ and $\Gamma(s)$ are given by (11) and (12), respectively.

Then following the inversion of (14):

$$\begin{bmatrix} \omega_1(s) \\ \omega_2(s) \end{bmatrix} = \begin{bmatrix} \zeta_1 w_1(s) + \gamma_2(s) \\ \zeta_1 (w_1^2(s)-1)^{1/2} \end{bmatrix} \frac{T_1(s)}{\Delta_1(s)} \quad (15)$$

where in (15):

$$\Delta_1(s) = \zeta_1 (\gamma_1(s) + \gamma_2(s)) w_1(s) + \gamma_1(s) \gamma_2(s) + \zeta_1^2$$

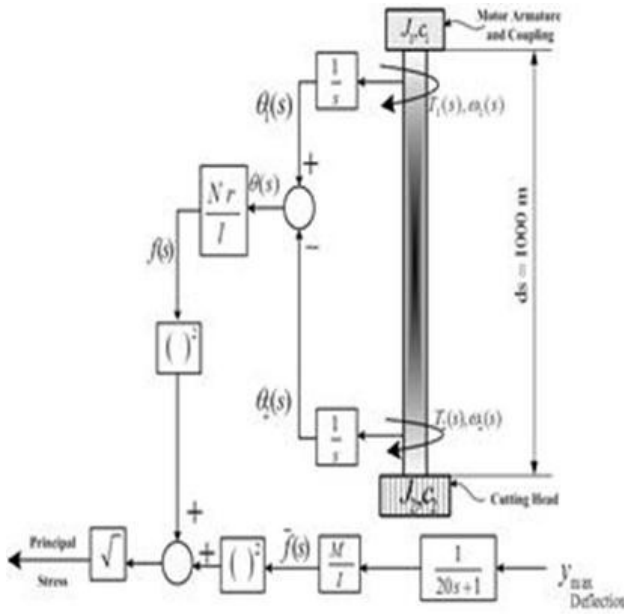


Fig. 3, Computation of Principal Stress

VI. APPLICATION STUDY

In this illustrative example, a ds which is 1000m long, 0.1682m outside diameter and 0.127 m inside diameter will be considered. The arrangement of the system is as shown in Fig. 3, where there are relatively lumped motor and cutting head inertia discs and per meter, ds gravitational loads, as in [11].

For this model:

$$J_1 = 3 \text{ kgm}^2, J_s (\text{shaft}) = 0.61359 \times 10^{-6}, J_2 = 3 \text{ kgm}^2,$$

$$c_1 = 1.0, c_2 = 100, 200 \text{ and } 300 \text{ Nmsec/rad}$$

$$l_1 = 1000\text{m}, r = 0.0738\text{m}, G_1 = 80 \times 10^9 \text{ N/m}^2, \rho_1 = 7800 \text{ kg/m}^3$$

$$\text{Hence: } \zeta = J_s \sqrt{(\rho G)} = 1323.94$$

$$\text{and } \Gamma(s) = s \sqrt{\left(\frac{\rho}{G}\right)} = 3.12 \times 10^{-4} \text{ sec}$$

The block diagram for the torsional, series form of (15) is as shown in Fig. 4. This block representation reflects the topology of the system enabling easy access to the ds dynamics and shaft shear stress transients.

Following a motor voltage input of $V = 100\text{v}$, the ds would be accelerated to 10 rad/sec, with $c_2 = 100 \text{ Nm sec/rad}$ as shown in Fig. 5. Correspondingly, the torsional stress, in the 1000 m long ds would increase to $1.4 \cdot 10^6 \text{ N/m}^2$, also shows the ds angular velocity, for increasing cutting load of 200 and 300 Nsec/rad with the ds velocity at the cutting head falling to approximately 5.0 and 3.4 rad/sec, respectively. Equally, the ds, steady state, torsional stress remains virtually constant, as would be expected, as the motor speed falls, in sympathy with the increasing, frictional cutting loads of 100, 200 and 300 N/(rad/sec), respectively. The ds twist angle for the above cutting conditions also remain virtually constant at 0.23 rad. However, any attempt to increase the cutting speed would result in proportional increases in the ds angular, deformation.

VII. PRINCIPAL STRESS COMPUTATION

Failure of the ds due to the combined bending- buckling, compression and torsional stresses may occur owing to fatigue following repeated loading cycles. Otherwise, rupture when exceeding the ds material yield point could occur with transient torque loading, at cutting start up, or with sudden rock cutting load disturbance increases, owing to the changing rock strata encountered.

An estimate for the principal dynamic stress can be simply achieved, as shown in Fig. 3, by assessing the ds twist angle. The compression and bending stresses are also available from the buckling analysis bending moment, of (1) and the ds deflection curves shown in Fig. 2. This assessment results in $M/I = 25 \times 10^9 \text{ N/m}^3$ and $Gr/l = 5.92 \times 10^6$.

The twisting, bending and delay dynamics are also included in the computation of the principal stress level, as shown in Fig. 6, where for $R = 0.02$ and $c_2 = 300 \text{ N/(rad/sec)}$, the maximum principal stress value reaches $250 \times 10^6 \text{ N/m}^2$. This is less than the elastic limit for steel, with the major loading contribution arising from the bending load.

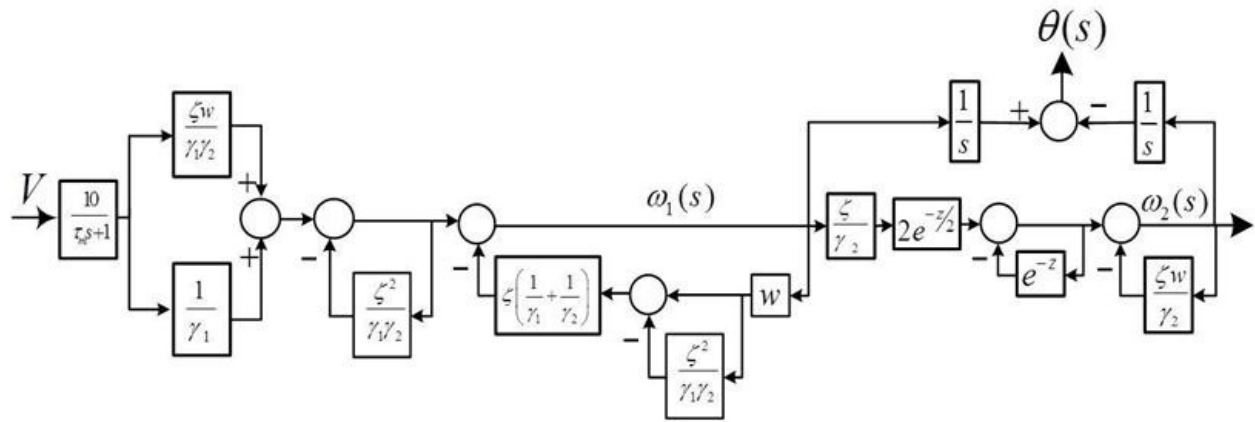
VIII. CONCLUSION

In this contribution, procedures enabling the determination of ds buckling and twisting under eccentric and ds mass, gravitational loading were considered. Torsional loading conditions, applied at the ds apex, were also included in the analysis ultimately enabling the principal stress concentration to be identified. Separate solutions for the ds bending / buckling configuration, based on the deflection of the structure, were incorporated whereas a lumped- distributed approach to the torsional problem, was invoked. This approach replicates the physical distortion of tubular ds where bending/ buckling and twisting distortion occur simultaneously, as a result of vertical compression and apex ds torque loading. The accumulated loading may ultimately manifest itself in the form of ds spiraling, along the whole length of the ds structure.

A series solution to the ds bending moment equation was proposed with appropriate boundary, termination conditions. Equally, the distributed - lumped parameter torsional model required the resolution of the continuous, partial differential equations, to achieve a compact solution.

To provide accurate results, in respect of the bending / buckling deflection, eccentric loading and the hydraulic bending moment which varies with borehole depth and annulus concentricity, was also included in the modeling process.

Owing to the requirement for a unique solution for the ds vertical loading model, inversion of the elastic, ds curve matrix was necessary. This confines the number of terms of the series solution producing thereby a simple polynomial representation for the ds deflection curve.



$$w = \frac{1 + e^{-z(s)}}{1 - e^{-z(s)}}, \quad z(s) = -2ls\sqrt{\frac{\rho}{G}}, \quad l = 1000 \text{ m},$$

$$\zeta = J_s\sqrt{(\rho G)}, \quad \tau_m = 10 \text{ sec}$$

$$\gamma_1 = J_1s + c_1 = 3s + 1$$

$$\gamma_2 = J_2s + c_2 = 3s + 100, 200 \text{ and } 300$$

Fig. 4, Distributed – Lumped Parameter Series Representation Of Drill String in Torsion

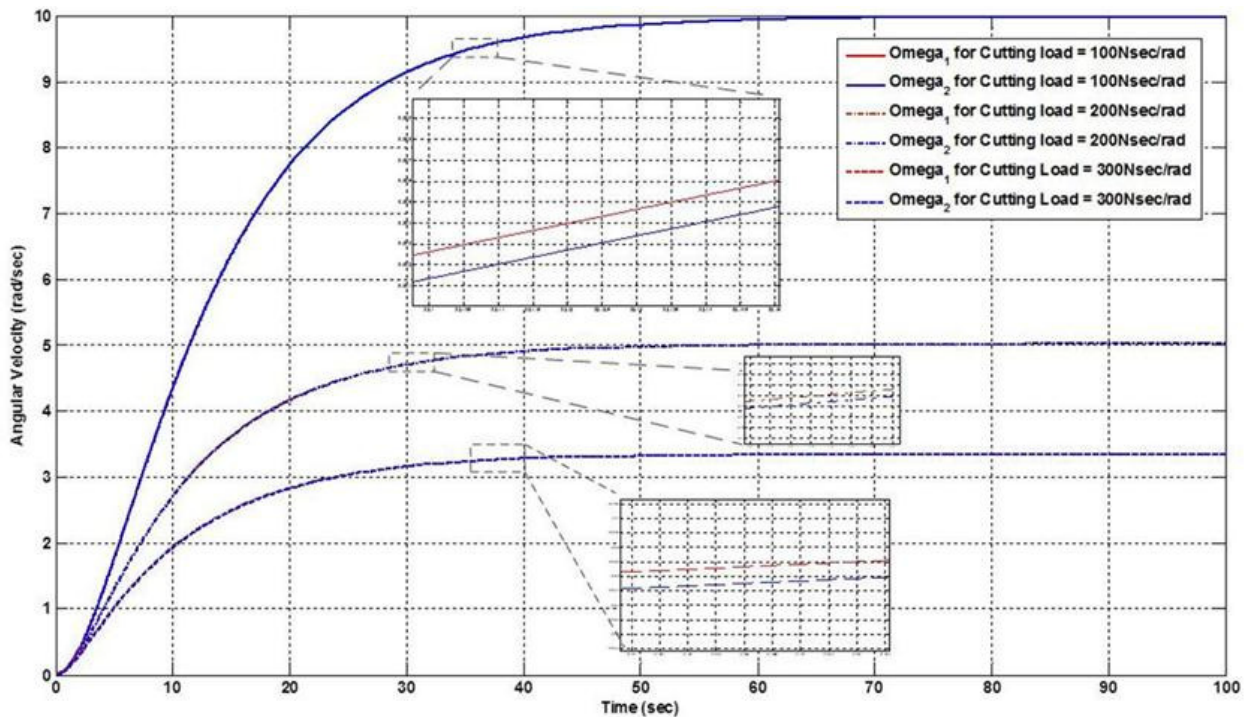


Fig. 5, Drill String Angular Velocity Increases Following Motor Step Voltage Change of 100 volts for Advancing Cutting Loads

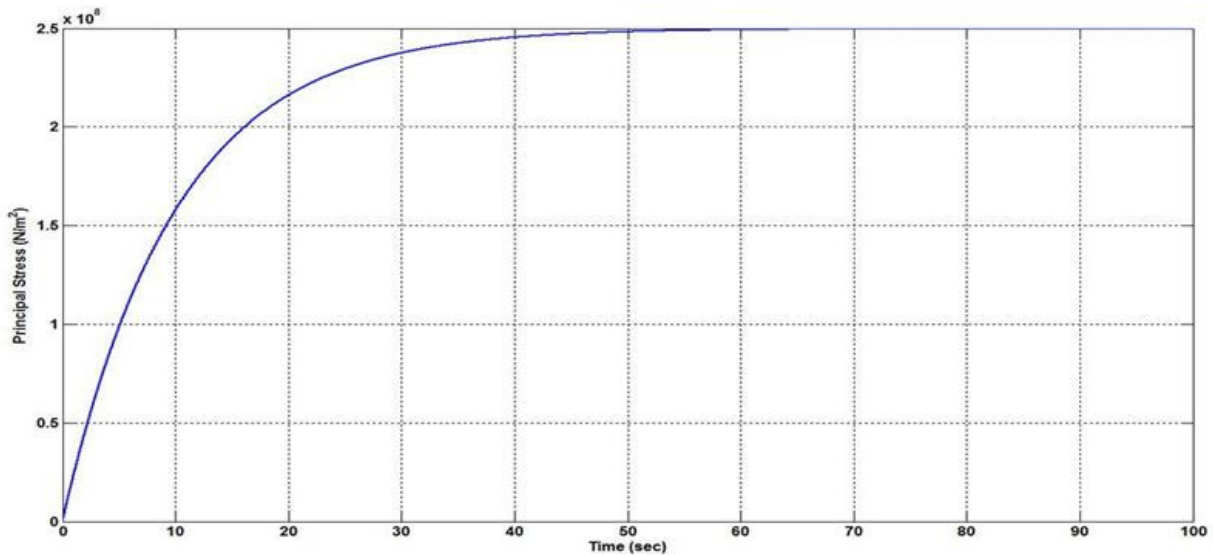


Fig. 6, Drill String Principal Stress Level Following Gradually Applied Loading with a Time Delay Approximately 20 sec for a Cutting load of 300 Nsec/rad

ACKNOWLEDGMENT

The author wishes to acknowledge the support and encouragement for this research provided by the Vice Chancellor, The British University in Dubai-UAE.

REFERENCES

- [1] F. S. Manning and R. E. Thompson, "Oil Field Processing of Petroleum", Penn Well Crop., Tulsa, 1991.
- [2] W. R. Tucker and C. Wang, "An Introduction for Drill String Dynamics", J. Sound and Vibration, vol. 224(1), 1999, pp 123-165.
- [3] A. Lubinski, "A Study of Buckling of Rotary Drill Strings", SPE spring Meeting, Oklahoma, 1950.
- [4] T. Huang and D. W. Dareing, "Buckling and Frequencies of Long Vertical Pipes", Proc. ASCE, vol. 95, no. EM1, 1969, pp 167-181.
- [5] A. Baryshnikov, A. Calderoni, A. Ligrone, P. Ferrara and S. P. A. Agip, "A New Approach to the Analysis of Drill String Fatigue Behavior", SPE 30524, Tech Conference, Dallas, 1998.
- [6] S. Rao, "Mechanical Vibrations", Addison Wesley, Reading, MA, 1985.
- [7] H. Rickardo, "A Modern Introduction to Differential Equations", Academic Press, London, 2009.
- [8] R. Bronson and G. B. Costa, "Differential Equations", McGraw-Hill, New York, 2009.
- [9] H. Rahnejat, "Multi-body Dynamics, Modeling and Simulation", IMechE., PEP Publishing, London, 1997.
- [10] R. S. Schwartz and B. Friedland, "Linear Systems", McGraw-Hill, New York, 1965.
- [11] H. Bartlett and R. Whalley, "Power Transmission System Modeling", Proc. IMechE., Pt. C, vol. 212, 1998, pp 497-508.